Guo et al. *Zool. Res.* 2026, 47(5): 1691−1702
https://doi.org/10.24272/j.issn.2095-8137.2025.447
https://cstr.cn/32248.14.zr.2025.447

ZR | Zoological Research

Article Open Access

A horizontally acquired gene mediates insect cocoon pigmentation in the eri silkmoth, *Samia ricini*

Hui-Duo Guo[1,2,#], Zhong-Jie Zhang[1,2,#], Ming-Fa Ling[1,2], Chen-Xin Sun[1], Yu Guo[1], Xiang-Biao Liu[1], Ke-Sen Zhu[3], Hui Xiang[3], He-Ying Qian[1,2,*], An-Jiang Tan[1,2,*]

[1] *Jiangsu Key Laboratory of Sericultural and Animal Biotechnology*, *School of Biotechnology*, *Jiangsu University of Science and Technology*, *Zhenjiang*, *Jiangsu* 212100, *China*

[2] *Key Laboratory of Silkworm and Mulberry Genetic Improvement*, *Ministry of Agriculture and Rural Affairs*, *The Sericultural Research Institute*, *Chinese Academy of Agricultural Sciences*, *Zhenjiang*, *Jiangsu* 212100, *China*

[3] *Guangdong Provincial Key Laboratory of Insect Developmental Biology and Applied Technology*, *Guangzhou Key Laboratory of Insect Development Regulation and Application Research*, *School of Life Sciences*, *South China Normal University*, *Guangzhou*, *Guangdong* 510631, *China*

ABSTRACT

Holometabolous insects make cocoons during larval–pupal metamorphosis to protect the pupal phase. The materials used for cocoon construction vary widely. Lepidopteran insects typically secrete silk to form cocoons, which display diverse colors. The eri silkworm, *Samia cynthia ricini*, is an economically important domesticated species that mostly produces white cocoons, with some varieties producing red cocoons. The enzyme kynureninase (KYNU), acquired from bacteria by horizontal gene transfer, has previously been implicated in insect coloration, while the tryptophan metabolite 3-hydroxyanthranilic acid (3-HAA) has been identified as a red pigment. However, exactly how *KYNU* is involved in cocoon pigmentation remains unclear. Here, we report that a horizontally transferred bacterial gene encoding *KYNU* regulates red cocoon formation. Metabolomic analysis revealed a high accumulation of 3-HAA in red cocoons, confirming its role as the primary pigment and associating the coloration with tryptophan metabolism. Quantitative real-time polymerase chain reaction (qPCR) analysis indicated that *SrKYNU* is highly expressed in the silk glands and significantly downregulated in the red cocoon strain compared to the white cocoon strain. Genomic sequencing identified a 141 bp deletion in the upstream regulatory region of *KYNU* in the red cocoon strain compared to the white cocoon strain. Dual-luciferase assays confirmed that this deletion significantly reduced promoter activity. CRISPR/Cas9 knockout of *SrKYNU* in the white-cocoon strain resulted in mutants producing red cocoons with elevated 3-HAA content. These findings reveal that the horizontally transferred gene *SrKYNU* exhibits tissue-specific expression and regulates cocoon coloration in *S. ricini*, illustrating that horizontal gene transfer can play an important role in regulating an insect physiological process.

Keywords: *Samia ricini*; Cocoon color; Horizontal gene transfer; Kynureninase; 3-hydroxyanthranilic acid

INTRODUCTION

Insects exhibit a variety of fascinating color patterns, which serve critical biological and ecological functions, including sexual selection, mimicry, camouflage, and warning coloration strategies that help them to disguise or hide from predators (Badejo et al., 2020; Caro et al., 2017; Figon & Casas, 2018). Insect coloration arises through multiple mechanisms, such as alterations in integumentary microstructures, shifts in refractive index, or variations in pigment composition (Moriyama, 2021; Shawkey & D'Alba, 2017). The pigments responsible for insect coloration are remarkably diverse, including endogenous pigments such as ommochromes (Figon & Casas, 2019), melanins (Popadić & Tsitlakidou, 2021), pteridines (Henze et al., 2019), purines (Fujii et al., 2020), bilins (Saito, 1998), as well as exogenous pigments such as flavonoids (Wilson, 1986) and carotenoids (Egorkin et al., 2024; Sakudoh et al., 2007).

Cocoon coloration represents a remarkable example among the diverse color patterns found in insects. While silk use is

This is an open-access article distributed under the terms of the Creative Commons Attribution Non-Commercial License (http://creativecommons.org/licenses/by-nc/4.0/), which permits unrestricted non-commercial use, distribution, and reproduction in any medium, provided the original work is properly cited.

Copyright ©2026 Editorial Office of Zoological Research, Kunming Institute of Zoology, Chinese Academy of Sciences

Received: 14 December 2025; Accepted: 22 January 2026; Online: 23 January 2026

Foundation items: This work was supported by the National Natural Science Foundation of China (32573304, 31925007, 32330102) and China Agriculture Research System of MOF and MARA (CARS-18)

[#]Authors contributed equally to this work

*Corresponding authors, E-mail: qianheying123@163.com; atan@just.edu.cn

widespread among insects, the silk cocoons from Lepidoptera species, particularly those from Bombycoidea silk moths, exhibit striking cocoon coloration and have attracted broad interest (Daimon et al., 2010; Leem et al., 2018; Lu et al., 2023; Sakudoh et al., 2007). Silk cocoons serve as a protective covering during the pupal stage. Studies on the Bombycidae species within this superfamily, specifically the domestic (*Bombyx mori*) and wild silkworms (*B. mandarina*), revealed that carotenoids and flavonoids are responsible for cocoon coloration. Carotenoids are responsible for the yellow–red series of cocoons (yellow, golden, orange, pink, flesh, and rust) (Tsuchida et al., 2004; Zhu & Zhang, 2014), while quercetin, a major flavonoid compound, accounts for green cocoons (Daimon et al., 2010). Extensive research has identified key genes involved in the uptake, transport, and regulation of these two pigments, as well as in cocoon coloration itself (Lu et al., 2023; Sakudoh et al., 2010; Tabunoki et al., 2004).

It is notable that species of Saturniidae (commonly known as giant silkmoths), which are evolutionary relatives of *Bombyx* silkworms, produce large cocoons exhibiting a diverse range of vibrant colors, with superior stability in color retention compared to those of *B. mori* (Dong et al., 2015; Reddy & Yang, 2010). Preliminary investigations on green-cocoon–spinning species of Saturniidae have detected endogenous pigments, such as bilins, in their cocoons (Leem et al., 2018; Yamada & Kato, 2004), suggesting that Saturniid silkmoths possess distinct mechanisms of cocoon coloration from those in *B. mori*. In Saturniidae, the eri silkmoth *Samia ricini* is a semi-domestic cocoon-spinning species. Because of its greater robustness under artificial rearing conditions compared to the silkworm *B. mori*, *S. ricini* has received increasing attention as another potential novel model of Lepidoptera (Lee et al., 2021; Lu et al., 2025; Peigler & Naumann, 2003). At present, several strains of *S. ricini* have been maintained. Most of them produce white cocoons, while one strain spins red cocoons, providing an ideal model for understanding cocoon coloration in insects.

In addition to the exogenous carotenoids reported in the yellow–red cocoons of *B. mori*, a few endogenous pigments such as ommochromes are also involved in red coloration (Ferré, 2024; Osanai-Futahashi et al., 2012, 2016). Ommochromes are synthesized from tryptophan metabolites, primarily 3-hydroxykynurenine (3-HK) and 3-hydroxyanthranilic acid (3-HAA), via the kynurenine pathway. These precursors are either taken up from the hemolymph or synthesized de novo within cells (Croce et al., 2024; Osanai-Futahashi et al., 2016; Uchiyama et al., 2023; Ze et al., 2021). This pathway is initiated by the conversion of tryptophan by tryptophan 2,3-dioxygenase (TDO) (Ahuja et al., 2023; Stone et al., 2013). Notably, the insect kynurenine pathway is incomplete compared to that in mammals, due to its lack of some key enzymes (Figon et al., 2020; Shamim et al., 2014). A prime example is the enzyme kynureninase (KYNU), which catalyzes the hydrolysis of kynurenine (KYN) and 3-hydroxykynurenine (3-HK) to produce anthranilic acid (AA) and 3-hydroxyanthranilic acid (3-HAA), respectively (Phillips, 2014). While *KYNU* is largely absent in insects, compelling evidence indicates it has been horizontally transferred from bacteria into several Lepidoptera species (Li et al., 2011; Sun et al., 2013; Zhu et al., 2011), suggesting that Lepidoptera species have evolved the capacity to produce 3-HAA and other derived pigments.

Diverse pigments can be synthesized through different branches of this pathway, contributing to considerable variation in both the key components and the mechanisms underlying red coloration. 3-HK is a precursor for the production of compound eye pigments during the pupal and early adult stages. Xanthurenic acid has previously been identified as a pigment in various hemimetabolous and holometabolous insects (Daniels & Reed, 2012). Through oxidative dimerization, 3-HAA and 3-HK give rise to cinnabarinic acid and xanthommatin, respectively (Fazio et al., 2017; Gawel, 2024). These pigments play a critical role in insect vision by enhancing contrast sensitivity and visual acuity (Figon & Casas, 2019; Thomas & Stocker, 1999). Given the complexity of the downstream metabolic processes involving 3-HAA (Dang et al., 2023), whether and how these pigments function in red cocoon coloration remains unclear.

In this study, we undertook a systematic investigation to reveal the mechanism regulating cocoon color in *S. ricini*. We first employed metabolomics to analyze the key metabolites of the white and red cocoons. Genomic sequencing was then used to identify causative genetic variations, followed by CRISPR/Cas9-mediated gene editing for functional validation. This work not only elucidates a novel mechanism of cocoon coloration in an emerging model Lepidoptera but also provides insights into the evolution of pigment biosynthesis through gene acquisition.

MATERIALS AND METHODS

Rearing of eri silkworm (*Samia ricini*)

The Baijian and Hongjian strains of *S. ricini* used in the study were obtained from the National Genetic Resources Bank of Silkworm in Jiangsu. The larvae of *S. ricini* were reared on fresh leaves of *Ricinus communis* provided twice daily under standard conditions at the Research Station of the Sericulture Institute, Jiangsu University of Science and Technology. Ambient temperature and relative humidity were maintained at 27±2°C and 80±10%, respectively, using an air-conditioned system. The Baijian strain is characterized by a white cocoon (W), while the Hongjian strain produces a red cocoon (R).

Untargeted liquid chromatography-tandem mass spectrometry (LC-MS/MS) detection and analysis

Eight individual cocoon samples per group, collected from the Baijian and Hongjian strains, were homogenized using a mechanical homogenizer. Methanol/acetonitrile solution was added to the homogenate for metabolite extraction. After centrifugation, the supernatant was dried in a vacuum centrifuge. For untargeted LC-MS/MS analysis, the dried samples were redissolved in an acetonitrile/water solvent. The analysis was performed using a UHPLC system (Agilent Technologies, USA) coupled to a quadrupole time-of-flight mass spectrometer (AB Sciex, Canada) at Shanghai Applied Protein Technology (China).

Quantification of tryptophan metabolites by targeted LC-MS/MS

Four cocoons per group from the Baijian and Hongjian strains were homogenized in pure acetonitrile spiked with deuterated internal standards (CDN Isotopes, Canada). Following centrifugation, the supernatants were diluted with deionized water before LC-MS/MS analysis. The analysis was performed on a Waters Acquity UPLC system with a C18-XB column. Detection was conducted on a TQ-XS mass spectrometer in

positive ion mode using optimized multiple reaction monitoring (MRM) transitions. Metabolites of the tryptophan pathway, including tryptophan, N-formylkynurenine, L-kynurenine, kynurenic acid, xanthurenic acid, 3-hydroxyanthranilic acid, 5-hydroxy-L-tryptophan, serotonin, melatonin, picolinic acid, tryptamine, indoleacetic acid, and indole-3-carboxaldehyde, were quantified using optimized MRM transitions. MassLynx software was used for data acquisition and processing. Calibration curves were established using deuterated analogs for each analyte to ensure quantification accuracy.

Reverse transcription-quantitative real-time polymerase chain reaction (RT-qPCR) detection

All tissues, including anterior silk gland (ASG), middle silk gland (MSG), posterior silk gland (PSG), Malpighian tubule (MT), fat body (FB), epithelium (E), and midgut (MG), were collected from day 5 fifth-instar larvae (L5D5) of the Baijian and Hongjian strains in cold physiological saline. One biological replicate consisted of tissues pooled from three silkworms, with a total of three biological replicates. Total RNA was extracted from all tissues using an EASYspin RNA Mini Kit (Aidlab Biotechnologies, China) according to the manufacturer's protocol. Genomic DNA was eliminated, and cDNA was synthesized from 1 μg of total RNA using the PrimeScript RT Reagent Kit with gDNA Eraser (Takara, Japan). qPCR was performed in triplicate using TB Green qPCR Master Mix (Takara, Japan) on a qPCR detection system (Thermo Fisher Scientific, USA). Primer sequences are listed in Supplementary Table S1. Gene expression was quantified using the comparative $2^{-\Delta\Delta Ct}$ method, with GAPDH as the endogenous control (Livak & Schmittgen, 2001; Vandesompele et al., 2002).

Whole genome resequencing

Genomic DNA was isolated from three individual male pupae of both the Baijian and Hongjian strains using the Genomic DNA Extraction Kit (Qiagen, Germany) according to the manufacturer's protocol. For whole genome resequencing, SMRTbell libraries were prepared using the SMRTbell Template Prep Kit 2.0 (Pacific Biosciences, USA) following standard protocols. Library quality was assessed using an Agilent 2100 Bioanalyzer (Agilent Technologies, USA). Qualified libraries were sequenced on the PacBio Sequel platform with a DNA Sequencing Kit 4.0 V2 at GrandOmics Biosciences (China). Raw reads were filtered by removing adapter sequences and low-quality reads. Reads with a minimum read length <500 bp or a minimum read quality score <0.75 were discarded. High-quality filtered reads were aligned to the reference *S. ricini* genome downloaded from InsectBase using SOAPaligner v.2.21 with default parameters.

Identification, verification, and annotation of structural variations

Structural variations (SVs) were identified using *Sniffles* (Sedlazeck et al., 2018) with default parameters. SV calls from 10 simulation replicates were merged using SURVIVOR software (Jeffares et al., 2017) with default parameters, requiring a minimum of 10 supporting reads for each SV call. To ensure high-confidence SV calls, we excluded SVs located in error-prone genomic regions (including 2.5 kb flanking sequences), those larger than 100 kb, and all calls with a reference genotype. To validate the quality of the identified SVs, we evaluated detection rates by analyzing SV calls across both sequenced strains. It should be noted that SV labels, including insertions, deletions, duplications, and inversions, were defined relative to the single reference genome and may not reflect the underlying mutation mechanisms. All filtered SVs were annotated using the GenomicRanges and ChIPseeker R packages to determine their overlap with various genomic features. To elucidate the potential biological significance of the population-stratified SVs, comprehensive functional enrichment analysis was performed. Kyoto Encyclopedia of Genes and Genomes (KEGG) pathway enrichment analysis was performed using the clusterProfiler R package (v.4.10.0). To account for multiple hypothesis testing, *P*-values were adjusted using the Benjamini–Hochberg false discovery rate (FDR) correction. Terms or pathways with an adjusted *P*-value (*Q*-value)<0.05 were regarded as statistically significant.

Cell transfection and Dual luciferase activity assay

To construct the luciferase reporter vector, we amplified the full-length 5' flanking region (2 000 bp) of the start codon of the *SrKYNU* gene from the genomes of both the Baijian and Hongjian strains. Purified PCR products were cloned into the *Bgl*II and *Hind*III restriction sites of the Renilla luciferase reporter vector pRL-TK, generating the recombinant plasmid pRL-KYNU. All primer sequences, including those containing the corresponding *Bgl*II and *Hind*III sites, are listed in Supplementary Table S1.

BmN cells derived from *B. mori* ovary were cultured in TC-100 medium (Gibco BRL, USA) supplemented with 10% fetal bovine serum at 26.5°C. At approximately 80% confluency, cells were co-transfected with 300 ng of each plasmid (pRL-KYNU and IE1-GL3) using GP-transfect-Mate transfection reagent (GenePharma, Beijing, China) according to the manufacturer's protocol. The IE1-GL3 reporter plasmid, which encodes firefly luciferase, served as an internal control for normalization. After 48 h, luciferase activities were quantified using the Dual-Luciferase Reporter Assay System (Promega, USA) following the manufacturer's instructions (Dual-lite Luciferase Assay Kit, Vazyme, China). Relative promoter activity was calculated as the ratio of Renilla luciferase activity (experimental reporter) to firefly luciferase activity (internal control). Three biological replicates were used in the experiment.

sgRNA/Cas9 Microinjection of *S. ricini* embryos

Two single guide RNAs (sgRNAs) targeting the *SrKYNU* gene (*Sric09765*) were designed using SnapGene software based on the $GGN_{18}NGG$ principle, with the PAM sequence included within the target region. To minimize the risk of off-target effects, we employed a strategy using multiple independent sgRNAs targeting different sites within the *SrKYNU* exon. Specific primers were designed across the potential off-target sites, and DNA sequencing was performed for the evaluation of the off-target effects. Each sgRNA template was generated using a unique oligonucleotide containing both the T7 promoter and target-specific sequence, followed by PCR amplification with Phanta Max Super-Fidelity DNA Polymerase (Vazyme, China). PCR products were cloned into the pJET1.2 blunt-end vector (Thermo Fisher Scientific, USA) and verified by sequencing. sgRNAs were synthesized using the Thermo Scientific Transcript Aid T7 High Yield Transcription Kit (Thermo Fisher Scientific, USA) and subsequently purified. The quality of the sgRNAs was assessed by agarose gel electrophoresis, and concentrations were measured using a NanoDrop One ultra-micro spectrophotometer.

Freshly laid embryos were collected for microinjection, which was completed within 6 hours after oviposition. The injection mixture contained Cas9 protein (300 ng/μL) and each sgRNA (500 ng/μL each). Microinjections were performed using a FemtoJet 4i microinjector coupled with an InjectMan 4 micromanipulation system (Eppendorf). Injected eggs were maintained at 25°C with appropriate humidity for 10 days to allow embryonic development and hatching.

Genotyping

Homozygous *SrKYNU* mutant strains were generated through successive generations of crossing. The abdominal feet of the adult moths were collected and stored at –25℃ for genomic DNA extraction using the EasyPure® Genomic DNA Kit (TransGen Biotech, China) according to the manufacturer's instructions. Target regions of *SrKYNU* were amplified using gene-specific primers with KOD FX Neo (Toyobo, Japan). The PCR procedure was as follows: one cycle of 94°C for 2 min, and 35 cycles of 94°C for 15 s, 55°C for 30 s, 68°C for 30 s, and one cycle of 68°C for 5 min. PCR products from G1–G3 individuals showing potential mutations were purified using the Gel Extraction Kit (Omega, USA) and subsequently cloned into the pJET1.2/blunt vector (Thermo, USA) for Sanger sequencing. Sequence analysis was performed to verify the specific mutation types (insertions or deletions) in each generation.

Phylogenetic analysis

To investigate the evolutionary origin of *SrKYNU*, we first used the protein sequence of KYNU as the query to perform a comprehensive BLASTP search against the NCBI non-redundant (nr) protein database. The BLASTP search was conducted with an E-value cutoff of 1×10^{-5}, while other parameters were kept at their default settings. The top 1 000 hits were retained for subsequent analyses. SrKYNU together with the retrieved KYNU homologs were subjected to phylogenetic analysis. Multiple amino acid sequence alignment was performed using MAFFT v.7.299 with the auto strategy (Katoh et al., 2002). Ambiguously aligned regions were subsequently trimmed using trimAl v.1.4 with the automated mode to improve alignment quality (Kalyaanamoorthy et al., 2017). Phylogenetic reconstruction was carried out using the maximum likelihood (ML) method implemented in IQ-TREE v.1.6.12, with automatic model selection enabled. Branch support was assessed using 1 000 ultrafast bootstrap replicates. The resulting phylogenetic tree was rooted using the midpoint rooting method. Phylogenetic trees were visualized using the iTOL online tool (http://itol.embl.de) (Letunic & Bork, 2019).

To further explore the evolutionary distribution of KYNU within Lepidoptera, we performed an additional BLASTP search against whole-genome protein datasets of lepidopteran species used in a previously published phylogenomic analysis (Gao et al., 2023), which allowed us to determine the presence and distribution of KYNU homologs in each lepidopteran genome. The detected KYNU protein IDs were manually mapped and annotated onto the species tree using Adobe Illustrator CS4.

Statistical analysis

All experiments were conducted with at least three biological replicates. Data are expressed as mean±standard error of the mean (SEM). For comparisons between two groups, a two-tailed unpaired Student's t-test was used. For comparisons involving multiple factors or time points, a two-way analysis of variance (ANOVA) was employed, followed by appropriate post-hoc tests. A P-value<0.05 was considered statistically significant. Statistical analyses were performed using GraphPad Prism v.8.

RESULTS

Tryptophan metabolism contributes to the red cocoon formation in *S. ricini*

Both the white (W) and red (R) cocoon strains exhibited a yellow plain phenotype in larval integument color (Figure 1A), but differed in cocoon color, with white for the W strain and red for the R strain (Figure 1B). To characterize the red cocoon pigment, untargeted liquid chromatography-tandem mass spectrometry (LC-MS/MS) was used to identify the differentially expressed metabolites between the W and R strains. Principal components analysis (PCA) disclosed substantial differences in cocoon metabolites between the W and R strains (Figure 1C). Metabolomic comparison showed that the R strain exhibited 30 up-regulated negative-ion (NEG) and 36 up-regulated positive-ion (POS) metabolites, along with 14 down-regulated NEG and 28 down-regulated POS metabolites relative to the W strain (Supplementary Figure S1). A volcano plot further revealed numerous differentially expressed metabolites between the W and R strains (adjusted P<0.05; variable importance in projection >1; Figure 1D). Analysis of the top 25 differentially expressed metabolites (Supplementary Figure S2) indicated significant accumulation of DL-tryptophan, 3-hydroxyanthranilic acid, and cinnabarinic acid in the R strain compared to the W strain (Figure 1D). KEGG pathway enrichment analysis demonstrated that these differentially expressed metabolites were primarily associated with fatty acid biosynthesis and tryptophan metabolism (Figure 1E). These findings showed that altered tryptophan metabolism contributes to red cocoon formation in *S. ricini*.

Accumulation of 3-hydroxyanthranilic acid is associated with red cocoon formation in *S. ricini*

To investigate the potential role of tryptophan metabolism in red cocoon formation, we conducted targeted LC–MS metabolomics analysis of tryptophan and its derivatives in the W and R strains (Supplementary Figure S3). The concentrations of 3-hydroxy-L-kynurenine (3-HK), xanthurenic acid, 3-hydroxyanthranilic acid (3-HAA, fold change=12), and cinnabarinic acid (fold change=400) in the kynurenine pathway were significantly higher in the R strain (Figure 2A). These findings strongly show that the increased accumulation of 3-HAA contributes to red pigmentation in *S. ricini* cocoons.

***SrKYNU* is specifically highly expressed in the posterior silk gland**

To elucidate tissue-specific expression patterns of tryptophan metabolic genes, we performed qPCR analyses of kynurenine pathway-related genes across multiple tissues, including ASG, MSG, PSG, MT, FB, E, and MG in both strains. As shown in Figure 2B, kynureninase (*SrKYNU*) was specifically highly expressed in PSG. Tryptophan 2,3-dioxygenase (*SrTDO*) mRNA expression in ASG and PSG of the Hongjian strain was higher than that in the Baijian strain (Figure 2C). Kynurenine formamidase (*SrKFM*) mRNA expression in MSG and PSG of the Hongjian strain was lower than that in the Baijian strain, while the mRNA expression of *SrKFM* in MT was higher (Figure 2D). Kynurenine 3-monooxygenase (*SrKMO*)

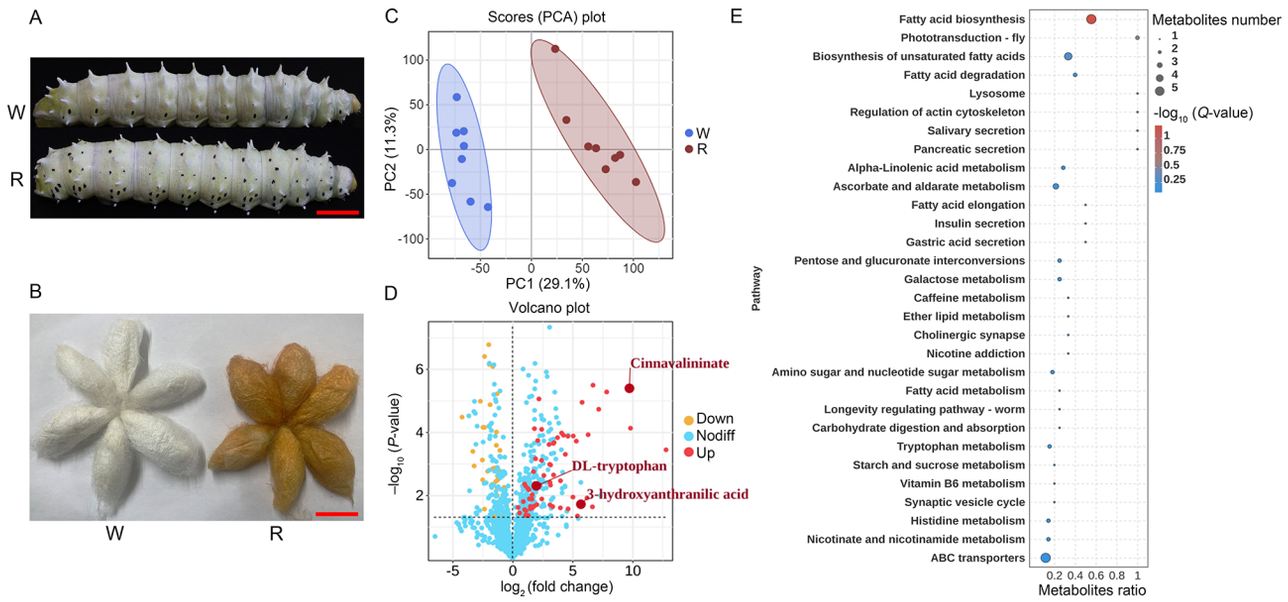


Figure 1 Graphical view and metabolome analysis of the white and red cocoon strains in *S. ricini*

A: Fifth instar larvae; scale bar: 10 mm. B: The white and brick-red cocoons in *S. ricini*. W: White cocoon strain; R: Red cocoon strain. Scale bar: 10 mm. C: The PCA plot of the white and red cocoon strains. D: Volcano plot showing the metabolites of the white and red cocoons. The red and orange dots in the figure represent differential metabolites, and the blue dots represent no significant difference (Nodiff). The orange dots represent the down-regulated metabolites, and the red dots represent the up-regulated metabolites. Red dots represent the most important up-regulated differential metabolites in the red cocoon vs. white cocoon. The x-axis corresponds to $\log_2$(fold change) and the y-axis corresponds to $-\log_{10}$(*P*-value). E: The differential metabolites enriched in KEGG pathways.

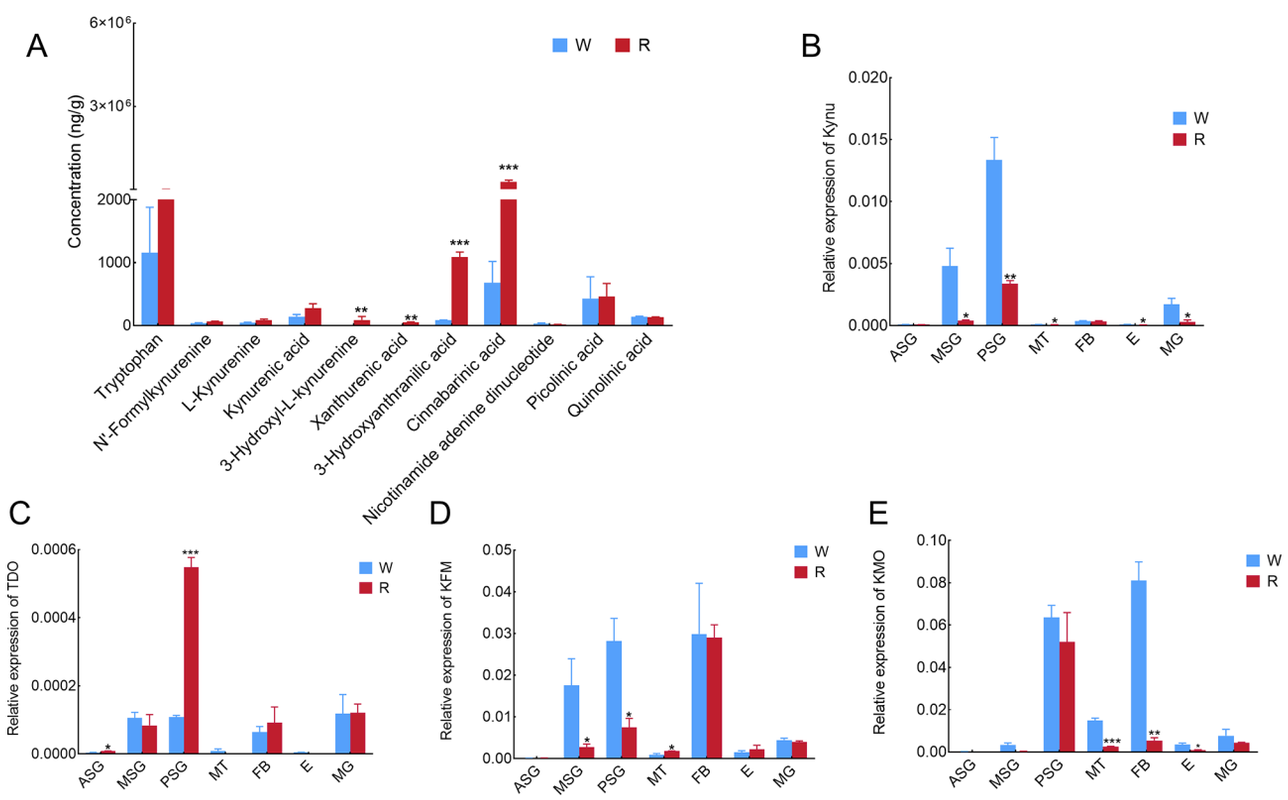


Figure 2 Tryptophan metabolites in white and red cocoons and their related gene expression in all tissues

A: The concentrations of tryptophan metabolites in white and red cocoons analyzed by targeted metabolomics. B–E: KYNU, TDO, KFM, and KMO mRNA expression in different tissues of *S. ricini*. *KYNU*, kynureninase; *TDO*, tryptophan 2,3-dioxygenase; *KFM*, kynurenine formamidase; and *KMO*, kynurenine 3-monooxygenase. Tissues tested were anterior silk gland (ASG), middle silk gland (MSG), posterior silk gland (PSG), Malpighian tubule (MT), fat body (FB), epithelium (E), and midgut (MG). Data are presented as mean±SEM. *: $P<0.05$; **: $P<0.01$; ***: $P<0.001$.

(Figure 2E) was predominantly expressed in FB compared to other tissues, and the mRNA expression in MT, FB, and E of the Hongjian strain was lower than that in the Baijian strain. Notably, the *SrKYNU* mRNA expression was significantly

down-regulated in the R strain compared with the W strain.

The red cocoon strain has a 141-bp deletion in the upstream regulatory sequence of *SrKYNU*

Structural variations (SVs), generally defined as genomic alterations affecting sequences >50 bp, play significant roles in evolution and phenotypic variation. A total of 36 486 putative SVs, including 17 419 insertions, 18 595 deletions, 206 inversions, and 266 duplications, were identified in the R strain, while 19 728 insertions, 20 917 deletions, 227 inversions, and 316 duplications were detected in the W strain (Supplementary Figure S4A). To investigate potential functional associations between SVs and cocoon coloration in *S. ricini*, we found that population-stratified SVs were enriched in fatty acid degradation (Supplementary Figure S4B). To validate the candidate gene, we examined its genomic region using the Integrative Genomics Viewer and identified a clear homozygous deletion, which was supported by a decreased read depth (Figure 3A, B). Notably, we conducted PCR amplification to identify a 141-bp deletion upstream of the tryptophan pathway-related gene *SrKYNU* in the red strain (Supplementary Figure S5). This finding suggests that *SrKYNU* is involved in red cocoon formation.

Dual luciferase reporter assays in BmN cells demonstrated significantly reduced promoter activity of the *SrKYNU* gene in the R strain compared to the W strain (Figure 3C). Taken together, these results indicate that the identified 141 bp region likely contributes to the downregulation of *SrKYNU* expression in the red cocoon strain.

CRISPR/Cas9-mediated *SrKYNU* knockout in *S. ricini* produces red cocoons with increased 3-HAA levels

To confirm the role of *SrKYNU* in red cocoon formation, we performed CRISPR/Cas9-mediated knockout of *SrKYNU* in the white cocoon strain. Two sgRNAs targeting exonic regions of *SrKYNU* were designed (Figure 4A). A total of 633 *S. ricini* embryos were injected, and the hatching rate was only 25.12% (Supplementary Tables S2). Following three generations of hybridization and screening, we obtained homozygous *SrKYNU* knockout (KO) mutants, carrying a 2 bp deletion, a 4 bp insertion, and a 1 bp mutation at the targeted locus, which led to a premature termination of translation (Supplementary Figure S6). KO mutants exhibited a distinct red cocoon phenotype (Figure 4B) and markedly reduced cocoon weight (Supplementary Figure S7). Tryptophan metabolites in the cocoons of KO and wild-type strains were quantified using targeted LC-MS/MS. A heatmap revealed that concentrations of multiple metabolites, including tryptophan, N-formylkynurenine, L-kynurenine, 3-hydroxy-L-kynurenine, xanthurenic acid, and 3-HAA, were increased in the *KO* strain compared with the wild (W) strain (Figure 4C). These findings demonstrate that the deletion of *SrKYNU* disrupts the tryptophan metabolic pathway, leading to accumulation of 3-HAA, which is responsible for the red cocoon phenotype in *S. ricini*.

***SrKYNU* is a horizontally transferred gene derived from bacteria**

The *SrKYNU* gene contains a 1 284 bp open reading frame (ORF) encoding a 428 amino acid protein, with no introns in its coding region. To investigate its evolutionary origin, we conducted a BLASTP search against the NCBI non-redundant protein database. Among the top 1 000 homologous sequences retrieved, all were exclusively derived from either Lepidoptera or Bacteria, with only one exception originating from Hemiptera. A phylogenetic analysis revealed that all lepidopteran KYNU proteins, including SrKYNU, formed a well-supported monophyletic clade (bootstrap value=98.6), indicating a single origin in a common lepidopteran ancestor. Crucially, the lepidopteran clade was robustly nested within a diversified bacterial clade (bootstrap value=93.5). This topological pattern provides direct evidence for horizontal acquisition (Figure 5). In contrast, a distant homolog from

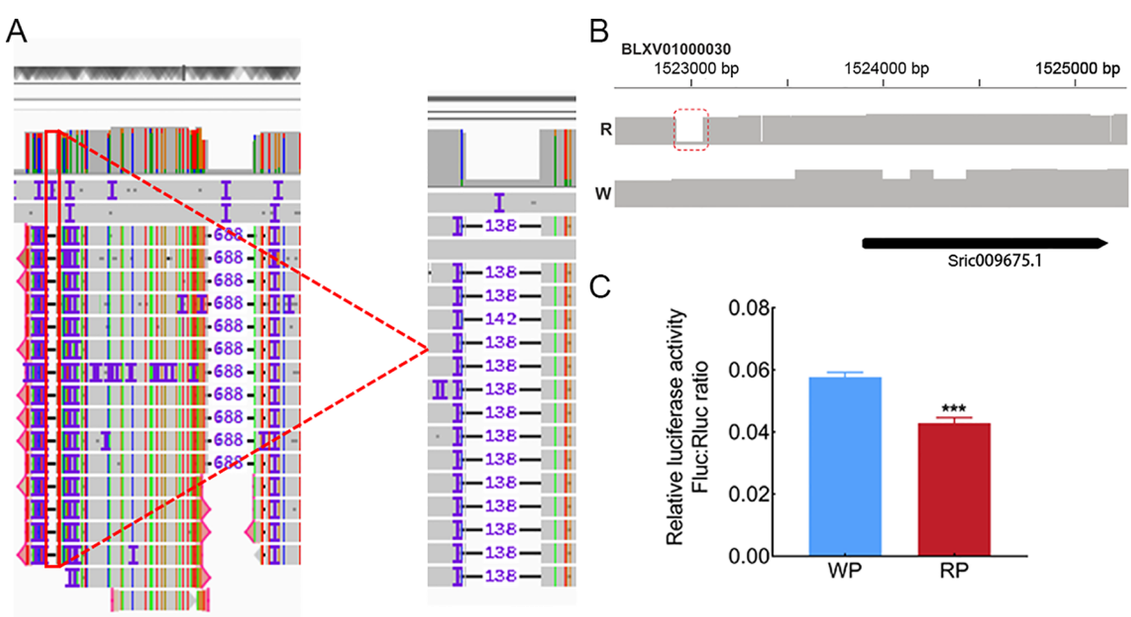


Figure 3 Whole-genome re-sequencing analysis and dual-luciferase activity assay in the white and red cocoon strains

A: The deletion upstream of *KYNU* in the red cocoon was identified by whole-genome re-sequencing and visualized with Integrative Genomics Viewer. B: The gene structure of KYNU in the white and red cocoons of *S. ricini*. C: Luciferase reporter assays in BmN cells transfected with reporter plasmids containing the promoters of KYNU from the white and red cocoons of *S. ricini*. The relative luciferase activity was normalized to Renilla luciferase/Firefly luciferase. Data are presented as mean±SEM. **: $P<0.01$.

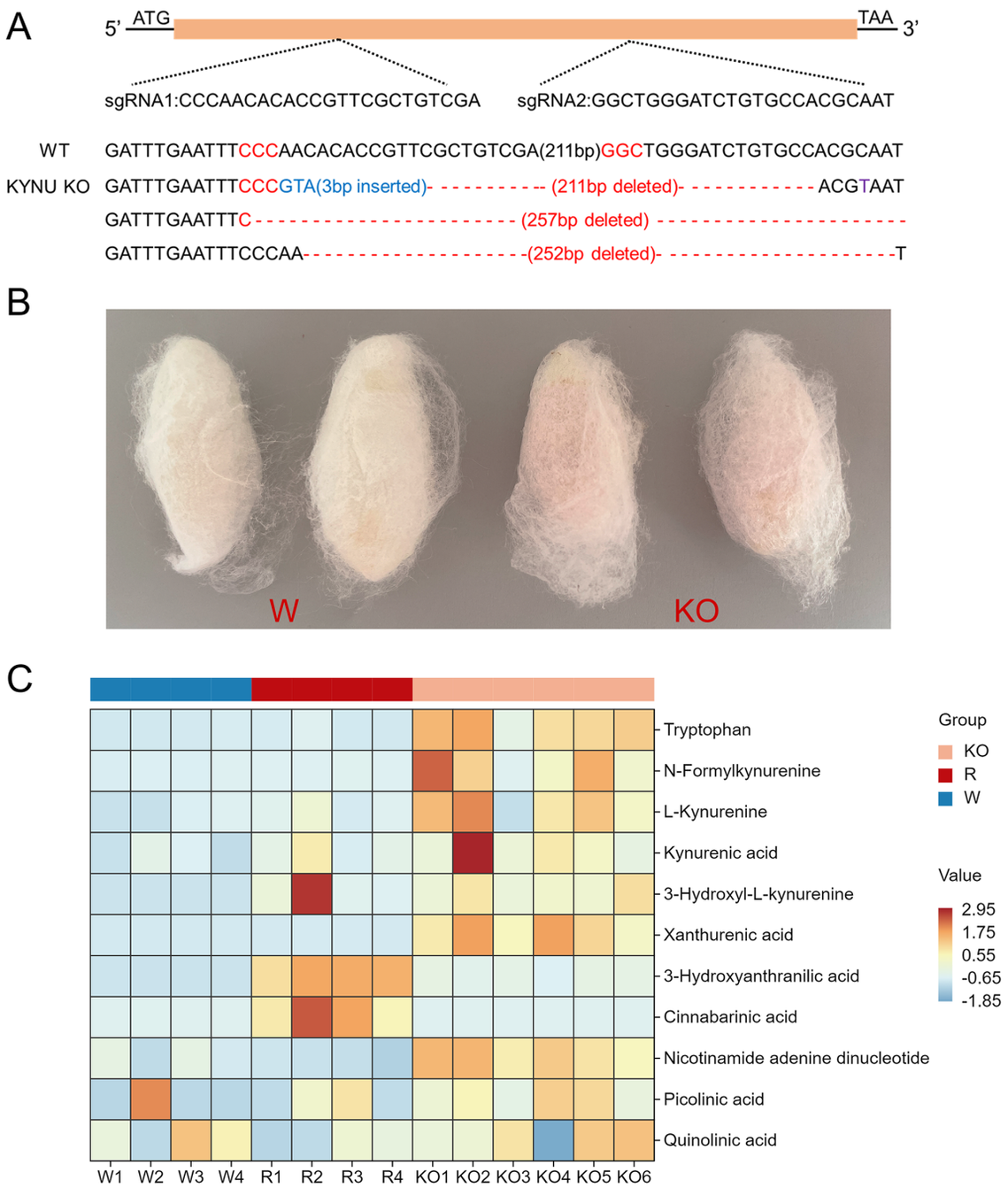


Figure 4 CRISPR/Cas9-based knockout of KYNU in the white cocoon strain

A: CRISPR/Cas9-based knockout of the *KYNU* gene. The two designed gRNAs are located in the exon of *KYNU*, indicated by dashed lines with target sequences. Target sequences of the two sgRNAs (black) and the protospacer adjacent motif (PAM) sequences (red). B: Cocoons of white and *KYNU* mutant *S. ricini*. C: Tryptophan metabolites in cocoons analyzed by targeted LC-MS/MS.

Hemiptera occupied a separate, basal position in the tree, indicating an independent horizontal gene transfer (HGT) event (Figure 5). These results demonstrate that *SrKYNU* has been acquired from bacteria via HGT.

KYNU is widespread in Lepidoptera

Phylogenetic analysis of *KYNUs* in Lepidoptera shows they are monophyletic, indicating a single origin. The distribution of *KYNUs* across Lepidoptera revealed their presence in multiple derived superfamilies, including Noctuoidea, Bombycoidea, Geometroidea, Pyraloidea, Papilionoidea, and Tortricoidea, while it was absent in the early-diverging lineages of Tineoidea. Divergence time estimation performed with PAML's MCMCTree using 46 lepidopteran species indicated that KYNU was not present in the ancestral Lepidoptera lineage (Figure 6). Instead, our findings support that KYNU was acquired through HGT by the common ancestor of Tortricoidea and subsequently retained in its descendant lineages.

DISCUSSION

Pigment formation in insects and cocoon metabolic insights in *S. ricini*

Insect pigmentation varies widely across species, developmental stages, and body regions. During cocoon

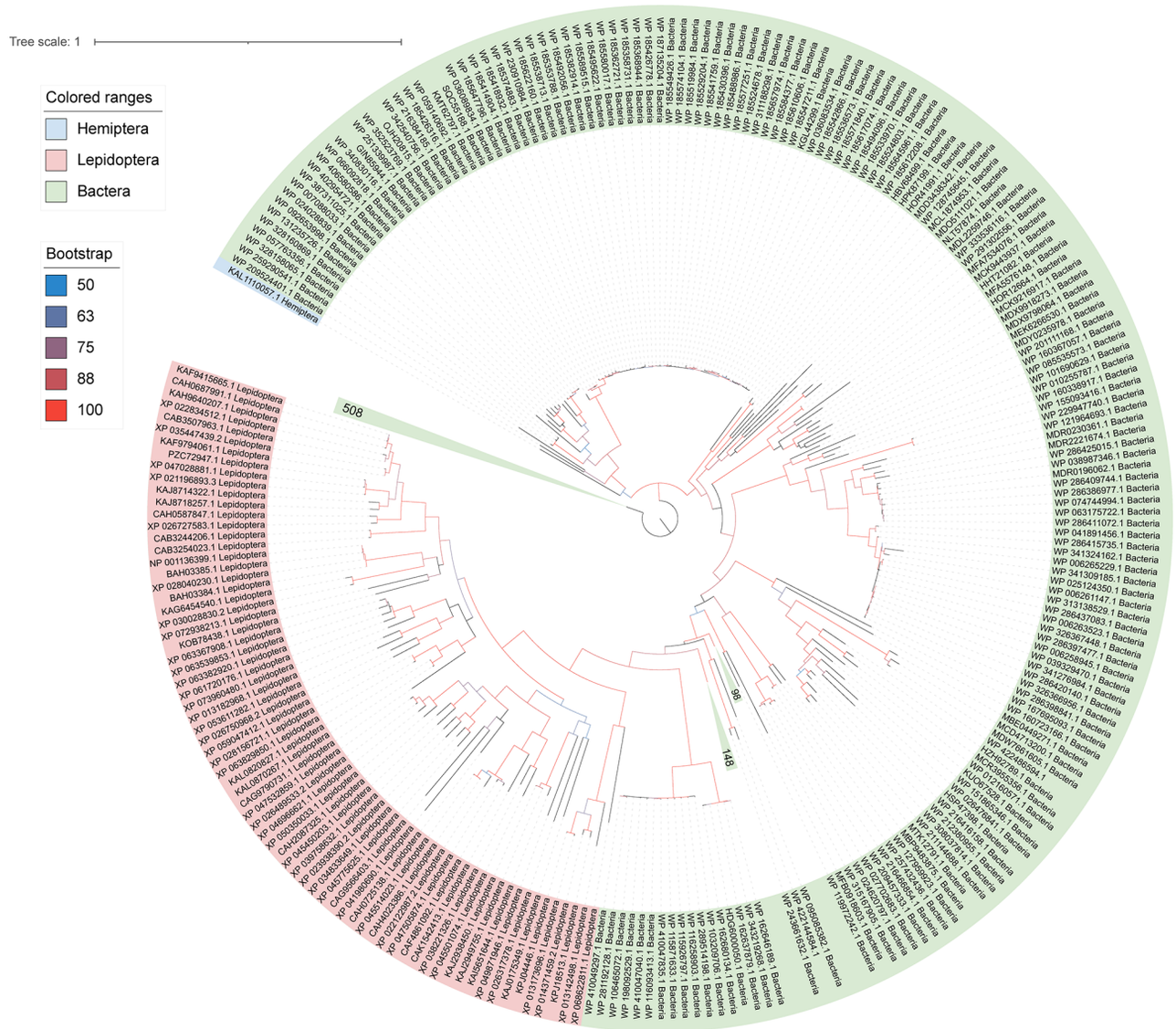


Figure 5 Phylogenetic evolutionary tree for the HGT-acquired gene *KYNU* from Lepidoptera, Bacteria, and Hemiptera

Multiple amino acid sequence alignment was performed using MAFFT v.7.299, trimmed in trimAl v.1.4, and analyzed in IQ-TREE v.1.6.12 with 1 000 bootstrap replicates. Tip colors denote taxonomic origin (pink: Lepidoptera; green: Bacteria; blue: Hemiptera). Node colors represent bootstrap support values.

formation, primary metabolites such as carbohydrates, proteins, and fat are primarily used for silk protein synthesis, while pigments are the key determinants of cocoon coloration. In the well-studied model *B. mori*, pigments are taken up by silk glands and bind to the silk protein; lastly, silk proteins bound with pigments are spun out by mature caterpillars to build colored cocoons. However, the mechanism in *S. ricini* appears to differ. We observed no pigment accumulation in the middle silk gland of the red cocoon strain *S. ricini*. A parallel phenomenon is observed in the *rb* mutant of *B. mori*, where ommochrome pigments accumulate in the hemolymph but only become visibly red upon exposure to air (Meng et al., 2009). Critically, *S. ricini* silk lacks L-fibroin (Lee et al., 2021). We suspect that a distinct pigment deposition mechanism in *S. ricini* likely requires exposure to air to develop its visible color. Our LC/MS-MS analysis revealed that the differentially expressed metabolites were primarily enriched in fatty acid synthesis and tryptophan metabolism between the white and red cocoon strains of *S. ricini*. Fatty acids, essential silk components, act as water repellents and enhance pupal survival under dry conditions (Zhang et al., 2017). This parallels the mechanism in *B. mori*, where specific lipophorins transport pigments to the silk gland in the colored strains, a capability absent in the white strains. Collectively, these observations indicate that tryptophan metabolism is likely involved in regulating cocoon color formation in *S. ricini*.

3-HAA is the main red pigment with dual physiological roles

White cocoons are characterized by the absence of the yellow pigments 3-hydroxykynurenine (3-HK) and xanthurenic acid (XA) (Daniels & Reed, 2012; Oxford & Gillespie, 1998). In contrast, the red cocoon strain of *S. ricini* accumulated 3-hydroxyanthranilic acid (3-HAA), a key tryptophan metabolite intermediate. We propose that the accumulation of 3-HAA is the primary determinant of red cocoon pigmentation, as its inherent red color directly corresponds to the observed cocoon pigmentation (Dang et al., 2023). Therefore, we propose that the accumulation of 3-HAA is the primary determinant of the red cocoon coloration in *S. ricini*. When 3-HK substitutes for 3-

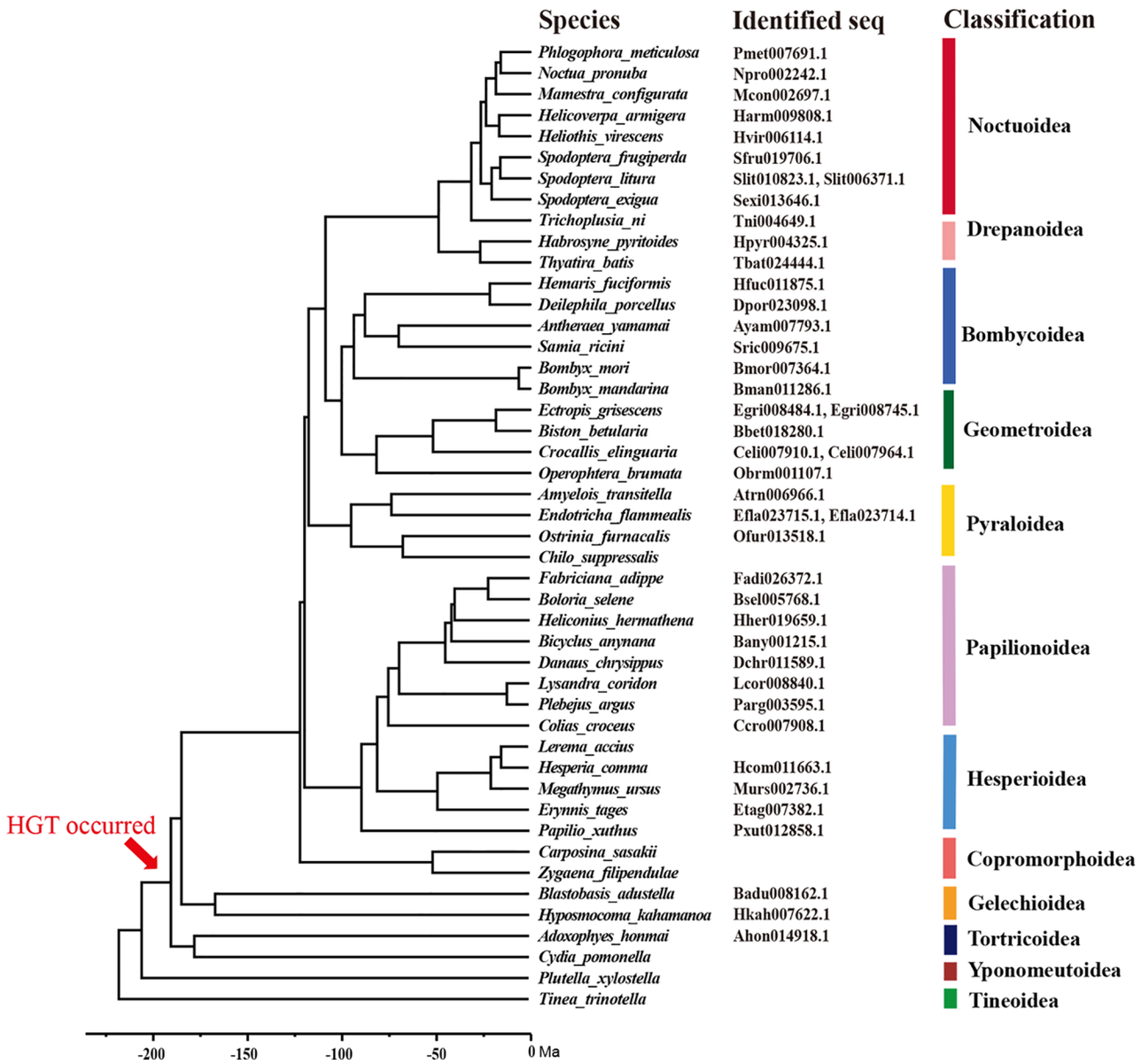


Figure 6 Ultrametric tree and contraction analysis of 46 lepidopteran species

The divergence time was estimated by MCMCTree, and the calibration time points were from TimeTree. Different superfamilies are indicated by vertical lines of different colors.

HAA in the metabolic pathway, the reaction yields reddish pigments in the absence of xanthommatin formation (Eggert et al., 1995; Soddu et al., 2004), consistent with the larval red body color in the *rb* mutant of *B. mori*, resulting from highly accumulated 3-HK (Meng et al., 2009). Notably, we also detected high levels of cinnabarinic acid (CA) in red cocoons. CA is a red phenoxazine derived from the condensation of two molecules of 3-HAA (Gawel, 2024; Meng et al., 2022). The presence of CA is consistent with an active 3-HAA metabolic flux and may represent a secondary stabilization or side product of the pigmentation pathway, though its quantitative contribution requires further study.

In addition to their roles in pigmentation, 3-HK and 3-HAA exhibit opposing physiological effects. 3-HK displays concentration-dependent redox activity. It acts as an antioxidant and can scavenge reactive oxygen species (ROS) at low levels, but promotes ROS generation and associated cytotoxicity at high concentrations or under oxidative stress, with links to neurotoxicity (Buchanan et al., 2023; Reyes-Ocampo et al., 2015). In contrast, 3-HAA demonstrates protective effects against oxidative stress by degrading hydrogen peroxide and activating the Nrf2/SKN-1 pathway, even extending lifespan in aging mice (Dang et al., 2023). Therefore, we propose that the accumulation of 3-HAA in *S. ricini* may help protect the pupa against oxidative stress during development.

A horizontally transferred gene *SrKYNU* with tissue-specific expression and functional divergence

The elevated 3-HAA levels observed in the red cocoon strain are likely driven by altered activity of key tryptophan-metabolizing enzymes. While KYNU is largely absent in insects, compelling evidence indicates it was horizontally transferred from bacteria into several Lepidoptera species. In *B. mori*, the HGT-acquired gene *BmKYNU*, originating from *Listeria grayi*, is predominantly expressed in Malpighian tubules and participates in detoxification. A single point mutation (T102I) in *BmKYNU* markedly reduces enzyme

activity, resulting in 3-HK accumulation and the red larval skin phenotype (Meng et al., 2009), illustrating how HGT-derived genes can influence insect pigmentation and supporting the role of HGT in facilitating ecological adaptation, including body coloration (Moran & Jarvik, 2010), detoxification (Wybouw et al., 2014), defense (Di Lelio et al., 2019), metabolism (Dai et al., 2021), and courtship behavior (Li et al., 2022).

In this study, we identified *SrKYNU* as a bacterial-derived HGT gene widespread across Lepidoptera, with an estimated divergence time of approximately 240 million years. Unlike *BmKYNU, SrKYNU* is predominantly expressed in the posterior silk gland (PSG) of *S. ricini*. This tissue-specific expression pattern indicates that the PSG serves as the primary site for tryptophan metabolite processing in *S. ricini*. This tissue-specific repurposing of an ancient HGT-acquired gene underscores how expression shifts can drive functional innovation.

The evolutionary trajectory of *KYNU* further reveals its role as a source of genetic material for lineage-specific adaptation. Notably, lepidopteran *KYNU* genes, including *SrKYNU*, lack introns. Although maintained across Lepidoptera, *KYNU* appears non-essential. Its loss is non-lethal in mosquitoes, and mutants in *B. mori* and *S. ricini* show no severe developmental defects, suggesting it resides in a genomic region under low selective pressure. During evolution, genomic rearrangements or other mutational events such as insertions (Miao et al., 2023), deletions, or point mutations could significantly alter expression patterns without major fitness costs, enabling the co-option of KYNU for diverse phenotypes. We hypothesize that *SrKYNU* regulates red cocoon formation by modulating 3-HAA levels. The red cocoon may have been shaped by selection for camouflage, UV protection, or pathogen defense, though its adaptive significance remains to be tested.

Genetic disruption of *SrKYNU* drives red cocoon formation via altered tryptophan flux

We found that *SrKYNU* mRNA expression is significantly reduced in the red cocoon strain. Whole-genome resequencing revealed a 141 bp deletion in the upstream regulatory region of *SrKYNU* in the red cocoon strain, which downregulates promoter activity and likely contributes to this transcriptional decrease. Consistent with models of KYNU deficiency in *B. mori* (Meng et al., 2009), the red-cocoon strain exhibited elevated levels of 3-HK compared to the white-cocoon strain, supporting a disruption in the conversion of 3-HK to 3-HAA.

In contrast to mammals, in which functional impairment of KYNU typically results in the accumulation of the toxic intermediate 3-HK, many insects naturally lack KYNU and have evolved alternative metabolic pathways for 3-HK disposal, such as transamination to xanthurenic acid (Croce et al., 2024). In *S. ricini*, residual *SrKYNU* activity, together with kynurenine aminotransferase (KAT), an enzyme conserved from mosquitoes to mammals (Han et al., 2007), catalyzes further kynurenine conversion into kynurenic acid. It may also maintain partial metabolic flux from 3-HK toward 3-HAA and xanthurenic acid, modulating intermediate accumulation and pigment outcome.

To establish a direct causal link, we performed CRISPR/Cas9-mediated knockout of *SrKYNU* in the white-cocoon strain. The decreased hatching rates after CRISPR/Cas9 gene editing, which is attributed to exogenously injected sgRNA influencing embryonic differentiation, are consistent with previous studies in silkworm (Hong et al., 2020). Due to the inherent challenges associated with microinjection in *S. ricini*, our sample size was insufficient for a statistically meaningful assessment of most traits. Fortunately, this genetic intervention successfully induced red-cocoon formation, with reduced cocoon weight. The elevated 3-HAA levels in the *SrKYNU* knockout mutants might be due to regulatory feedback within the pathway, confirming that reduced *SrKYNU* function is sufficient to trigger the red-pigmentation phenotype. These results demonstrate that an upstream deletion in *SrKYNU* attenuates its expression, leading to metabolic reprogramming of the tryptophan pathway and red cocoon formation.

From an applied perspective, red cocoons currently hold limited direct economic value, as white cocoons dominate commercial eri silk production, largely because the red pigment is unstable and washed out during standard silk processing. Nevertheless, by elucidating the genetic basis of this coloration, our study can provide a foundation for future efforts to stabilize the pigment, potentially enabling novel applications in advanced textiles or biomaterials.

In summary, our study establishes a clear causal pathway underlying red cocoon formation in *S. ricini*. We demonstrate that reduced expression of *SrKYNU* affects the conversion of 3-HK to 3-HAA and leads to the accumulation of the red pigment 3-HAA. CRISPR/Cas9-mediated disruption of *SrKYNU* in the white cocoon strain successfully recapitulated the red cocoon phenotype, confirming that loss of *SrKYNU* function is both necessary and sufficient to trigger this coloration phenotype. These findings provide compelling evidence that a horizontally transferred bacterial gene encoding *SrKYNU* plays a critical role in regulating cocoon pigmentation in *S. ricini*, and that its functional impairment is responsible for its red cocoon color.

DATA AVAILABILITY

The original raw reads from Illumina sequencing can be downloaded from the NCBI (PRJNA1510321), China National Center for Bioinformation (PRJCA069640), and Science Data Bank (https://www.scidb.cn/) under DOI: 10.57760/sciencedb.j00139.000bd.

SUPPLEMENTARY DATA

Supplementary data to this article can be found online.

COMPETING INTERESTS

The authors declare that they have no competing interests.

AUTHORS' CONTRIBUTIONS

H.D.G. and A.J.T. designed the original research; H.D.G. and Z.J.Z. performed the research; H.Y.Q. and A.J.T. contributed reagents and analytic tools; H.D.G., Z.J.Z., M.F.L., C.X.S., Y.G., X.B.L., K.S.Z., H.X., H.Y.Q., and A.J.T. drafted the manuscript; H.D.G., H.X., and A.J.T. revised the manuscript. All authors read and approved the final version of the manuscript.

ACKNOWLEDGMENTS

We thank Dr. Han Gao from the Jiangsu University of Science and Technology for the data analysis.

REFERENCES

Ahuja N, Hwaun E, Pungor JR, et al. 2023. Creation of an albino squid line by CRISPR-Cas9 and its application for *in vivo* functional imaging of neural activity. *Current Biology*, **33**(13): 2774–2783. e5.

Badejo O, Skaldina O, Gilev A, et al. 2020. Benefits of insect colours: a review from social insect studies. *Oecologia*, **194**(1-2): 27–40.

Buchanan JL, Rauckhorst AJ, Taylor EB. 2023. 3-hydroxykynurenine is a ROS-inducing cytotoxic tryptophan metabolite that disrupts the TCA cycle. *BioRxiv*, doi: https://doi.org/10.1101/2023.07.10.548411.

Caro T, Stoddard MC, Stuart-Fox D. 2017. Animal coloration research: why it matters. *Philosophical Transactions of the Royal Society B: Biological Sciences*, **372**(1724): 20160333.

Croce AC, Garbelli A, Moyano A, et al. 2024. Developmental and nutritional dynamics of malpighian tubule autofluorescence in the asian tiger mosquito *Aedes albopictus*. *International Journal of Molecular Sciences*, **25**(1): 245.

Dai XP, Kiuchi T, Zhou YY, et al. 2021. Horizontal gene transfer and gene duplication of β-fructofuranosidase confer lepidopteran insects metabolic benefits. *Molecular Biology and Evolution*, **38**(7): 2897–2914.

Daimon T, Hirayama C, Kanai M, et al. 2010. The silkworm *Green b* locus encodes a quercetin 5-*O*-glucosyltransferase that produces green cocoons with UV-shielding properties. *Proceedings of the National Academy of Sciences of the United States of America*, **107**(25): 11471–11476.

Dang H, Castro-Portuguez R, Espejo L, et al. 2023. On the benefits of the tryptophan metabolite 3-hydroxyanthranilic acid in *Caenorhabditis elegans* and mouse aging. *Nature Communications*, **14**(1): 8338.

Daniels EV, Reed RD. 2012. Xanthurenic acid is a pigment in *Junonia coenia* butterfly wings. *Biochemical Systematics and Ecology*, **44**: 161–163.

Di Lelio I, Illiano A, Astarita F, et al. 2019. Evolution of an insect immune barrier through horizontal gene transfer mediated by a parasitic wasp. *PLoS Genetics*, **15**(3): e1007998.

Dong Y, Dai FY, Ren YD, et al. 2015. Comparative transcriptome analyses on silk glands of six silkmoths imply the genetic basis of silk structure and coloration. *BMC Genomics*, **16**(1): 203.

Eggert C, Temp U, Dean JFD, et al. 1995. Laccase-mediated formation of the phenoxazinone derivative, cinnabarinic acid. *FEBS Letters*, **376**(3): 202–206.

Egorkin NA, Dominnik EE, Maksimov EG, et al. 2024. Insights into the molecular mechanism of yellow cuticle coloration by a chitin-binding carotenoprotein in gregarious locusts. *Communications Biology*, **7**(1): 448.

Fazio F, Lionetto L, Curto M, et al. 2017. Cinnabarinic acid and xanthurenic acid: two kynurenine metabolites that interact with metabotropic glutamate receptors. *Neuropharmacology*, **112**: 365–372.

Ferré J. 2024. Biosynthesis of pteridines in insects: a review. *Insects*, **15**(5): 370.

Figon F, Casas J. 2018. Morphological and physiological colour changes in the animal kingdom. *In*: Encyclopedia of Life Sciences. Chichester: John Wiley & Sons, Ltd. , 1–11.

Figon F, Casas J. 2019. Ommochromes in invertebrates: biochemistry and cell biology. *Biological Reviews*, **94**(1): 156–183.

Figon F, Munsch T, Croix C, et al. 2020. Uncyclized xanthommatin is a key ommochrome intermediate in invertebrate coloration. *Insect Biochemistry and Molecular Biology*, **124**: 103403.

Fujii T, Kakino K, Tanaka M, et al. 2020. A defect in purine nucleotide metabolism in the silkworm, *Bombyx mori*, causes a translucent larval integument and male infertility. *Insect Biochemistry and Molecular Biology*, **126**: 103458.

Gao H, Li YX, Tian Y, et al. 2023. Gene family expansion analysis and identification of the histone family in *Spodoptera frugiperda*. *Comparative Biochemistry and Physiology Part D: Genomics and Proteomics*, **48**: 101142.

Gawel K. 2024. A review on the role and function of cinnabarinic acid, a “forgotten” metabolite of the kynurenine pathway. *Cells*, **13**(5): 453.

Han Q, Beerntsen BT, Li JY. 2007. The tryptophan oxidation pathway in mosquitoes with emphasis on xanthurenic acid biosynthesis. *Journal of Insect Physiology*, **53**(3): 254–263.

Henze MJ, Lind O, Wilts BD, et al. 2019. Pterin-pigmented nanospheres create the colours of the polymorphic damselfly *Ischnura elegans*. *Journal of the Royal Society Interface*, **16**(153): 20180785.

Hong JW, Jeong CY, Yu JH, et al. 2020. *Bombyx mori* kynurenine 3-monooxygenase gene editing and insect molecular breeding using the clustered regularly interspaced short palindromic repeat/CRISPR associated protein 9 system. *Biotechnology Progress*, **36**(6): e3054.

Jeffares DC, Jolly C, Hoti M, et al. 2017. Transient structural variations have strong effects on quantitative traits and reproductive isolation in fission yeast. *Nature Communications*, **8**: 14061.

Kalyaanamoorthy S, Minh BQ, Wong TKF, et al. 2017. ModelFinder: fast model selection for accurate phylogenetic estimates. *Nature Methods*, **14**(6): 587–589.

Katoh K, Misawa K, Kuma KI, et al. 2002. MAFFT: a novel method for rapid multiple sequence alignment based on fast Fourier transform. *Nucleic Acids Research*, **30**(14): 3059–3066.

Lee J, Nishiyama T, Shigenobu S, et al. 2021. The genome sequence of *Samia ricini*, a new model species of lepidopteran insect. *Molecular Ecology Resources*, **21**(1): 327–339.

Leem JW, Allcca AEL, Chen JJ, et al. 2018. Visible light biophotosensors using biliverdin from *Antheraea yamamai*. *Optics Express*, **26**(24): 31817–31828.

Letunic I, Bork P. 2019. Interactive tree of life (iTOL) v4: recent updates and new developments. *Nucleic Acids Research*, **47**(W1): W256–W259.

Li Y, Liu ZG, Liu C, et al. 2022. HGT is widespread in insects and contributes to male courtship in lepidopterans. *Cell*, **185**(16): 2975–2987. e10.

Li ZW, Shen YH, Xiang ZH, et al. 2011. Pathogen-origin horizontally transferred genes contribute to the evolution of Lepidopteran insects. *BMC Evolutionary Biology*, **11**: 356.

Livak KJ, Schmittgen TD. 2001. Analysis of relative gene expression data using real-time quantitative PCR and the $2^{-\Delta\Delta Ct}$ method. *Methods*, **25**(4): 402–408.

Lu KP, Shen JH, Huang WG, et al. 2025. Chromosome-level genome and variation map of eri silkworm samia *Cynthia Ricini*. *Biology (Basel)*, **14**(6): 698.

Lu YR, Luo JW, An ER, et al. 2023. Deciphering the genetic basis of silkworm cocoon colors provides new insights into biological coloration and phenotypic diversification. *Molecular Biology and Evolution*, **40**(2): msad017.

Meng D, Shao X, Luo SP, et al. 2022. Pigment production by a newly isolated strain *Pycnoporus sanguineus* SYBC-L7 in solid-state fermentation. *Frontiers in Microbiology*, **13**: 1015913.

Meng Y, Katsuma S, Mita K, et al. 2009. Abnormal red body coloration of the silkworm, *Bombyx mori*, is caused by a mutation in a novel kynureninase. *Genes to Cells*, **14**(2): 129–140.

Miao YH, Huang DW, Xiao JH. 2023. Complicated expansion trajectories of insertion sequences and potential association with horizontal transfer of Wolbachia DNA. *Zoological Research*, **44**(2): 273–275.

Moran NA, Jarvik T. 2010. Lateral transfer of genes from fungi underlies carotenoid production in aphids. *Science*, **328**(5978): 624–627.

Moriyama M. 2021. Physiological and biochemical mechanisms of insect color change towards understanding molecular links. *In*: Hashimoto H, Goda M, Futahashi R, Kelsh T, Akiyama T. Pigments, Pigment Cells and Pigment Patterns. Singapore: Springer, 451–472.

Osanai-Futahashi M, Tatematsu KI, Futahashi R, et al. 2016. Positional cloning of a *Bombyx pink-eyed* white egg locus reveals the major role of *cardinal* in ommochrome synthesis. *Heredity (Edinb)*, **116**(2): 135–145.

Osanai-Futahashi M, Tatematsu KI, Yamamoto K, et al. 2012. Identification of the *Bombyx red egg* gene reveals involvement of a novel transporter family gene in late steps of the insect ommochrome biosynthesis pathway.

Journal of Biological Chemistry, **287**(21): 17706–17714.
Oxford GS, Gillespie RG. 1998. Evolution and ecology of spider coloration. *Annual Review of Entomology*, **43**: 619–643.
Peigler RS, Naumann S. 2003. A Revision of the Silkmoth Genus Samia. San Antonio: University of the Incarnate Word.
Phillips RS. 2014. Structure and mechanism of kynureninase. *Archives of Biochemistry and Biophysics*, **544**: 69–74.
Popadić A, Tsitlakidou D. 2021. Regional patterning and regulation of melanin pigmentation in insects. *Current Opinion in Genetics & Development*, **69**: 163–170.
Reddy N, Yang YQ. 2010. Morphology and tensile properties of silk fibers produced by uncommon *Saturniidae*. *International Journal of Biological Macromolecules*, **46**(4): 419–424.
Reyes-Ocampo J, Ramírez-Ortega D, Vázquez Cervantes GI, et al. 2015. Mitochondrial dysfunction related to cell damage induced by 3-hydroxykynurenine and 3-hydroxyanthranilic acid: non-dependent-effect of early reactive oxygen species production. *NeuroToxicology*, **50**: 81–91.
Saito H. 1998. Purification and properties of two blue biliproteins from the larval hemolymph and integument of *Rhodinia fugax* (Lepidoptera: Saturniidae). *Insect Biochemistry and Molecular Biology*, **28**(12): 995–1005.
Sakudoh T, Iizuka T, Narukawa J, et al. 2010. A CD36-related transmembrane protein is coordinated with an intracellular lipid-binding protein in selective carotenoid transport for cocoon coloration. *Journal of Biological Chemistry*, **285**(10): 7739–7751.
Sakudoh T, Sezutsu H, Nakashima T, et al. 2007. Carotenoid silk coloration is controlled by a carotenoid-binding protein, a product of the *Yellow blood* gene. *Proceedings of the National Academy of Sciences of the United States of America*, **104**(21): 8941–8946.
Sedlazeck FJ, Rescheneder P, Smolka M, et al. 2018. Accurate detection of complex structural variations using single-molecule sequencing. *Nature Methods*, **15**(6): 461–468.
Shamim G, Ranjan SK, Pandey DM, et al. 2014. Biochemistry and biosynthesis of insect pigments. *European Journal of Entomology*, **111**(2): 149–164.
Shawkey MD, D'Alba L. 2017. Interactions between colour-producing mechanisms and their effects on the integumentary colour palette. *Philosophical Transactions of the Royal Society B: Biological Sciences*, **372**(1724): 20160536.
Soddu G, Sanjust E, Murgia S, et al. 2004. Interference of some tryptophan metabolites in the formation of melanin in vitro. *Pigment Cell Research*, **17**(2): 135–141.
Stone TW, Stoy N, Darlington LG. 2013. An expanding range of targets for kynurenine metabolites of tryptophan. *Trends in Pharmacological Sciences*, **34**(2): 136–143.
Sun BF, Xiao JH, He SM, et al. 2013. Multiple ancient horizontal gene transfers and duplications in lepidopteran species. *Insect Molecular Biology*, **22**(1): 72–87.
Tabunoki H, Higurashi S, Ninagi O, et al. 2004. A carotenoid-binding protein (CBP) plays a crucial role in cocoon pigmentation of silkworm (*Bombyx mori*) larvae. *FEBS Letters*, **567**(2-3): 175–178.
Thomas SR, Stocker R. 1999. Redox reactions related to indoleamine 2, 3-dioxygenase and tryptophan metabolism along the kynurenine pathway. *Redox Report*, **4**(5): 199–220.
Tsuchida K, Katagiri C, Tanaka Y, et al. 2004. The basis for colorless hemolymph and cocoons in the *Y*-gene recessive *Bombyx mori* mutants: a defect in the cellular uptake of carotenoids. *Journal of Insect Physiology*, **50**(10): 975–983.
Uchiyama H, Takasu Y, Moriyama M, et al. 2023. A novel monocarboxylate transporter involved in 3-hydroxykynurenine transport for ommochrome coloration. *BioRxiv*, doi: https://doi.org/10.1101/2023.06.01.543243.
Vandesompele J, De Preter K, Pattyn F, et al. 2002. Accurate normalization of real-time quantitative RT-PCR data by geometric averaging of multiple internal control genes. *Genome Biology*, **3**(7): Research0034.1.
Wilson A. 1986. Flavonoid pigments and wing color in *Melanargia galathea*. *Journal of Chemical Ecology*, **12**(1): 49–68.
Wybouw N, Dermauw W, Tirry L, et al. 2014. A gene horizontally transferred from bacteria protects arthropods from host plant cyanide poisoning. *eLife*, **3**: e02365.
Yamada H, Kato Y. 2004. Green colouration of cocoons in *Antheraea yamamai* (Lepidoptera: Saturniidae): light-induced production of blue bilin in the larval haemolymph. *Journal of Insect Physiology*, **50**(5): 393–401.
Ze LJ, Xu P, Kang WN, et al. 2021. Disruption of kynurenine pathway reveals physiological importance of tryptophan catabolism in *Henosepilachna vigintioctopunctata*. *Amino Acids*, **53**(7): 1091–1104.
Zhang Y, Zhao DC, Meng Z, et al. 2017. Wild silkworm cocoon contains more metabolites than domestic silkworm cocoon to improve its protection. *Journal of Insect Science*, **17**(5): 105.
Zhu B, Lou MM, Xie GL, et al. 2011. Horizontal gene transfer in silkworm, *Bombyx mori*. *BMC Genomics*, **12**: 248.
Zhu L, Zhang YQ. 2014. Identification and analysis of the pigment composition and sources in the colored cocoon of the silkworm, *Bombyx mori*, by HPLC-DAD. *Journal of Insect Science*, **14**(1): 31.